Heliyon 9 (2023) e17613

Contents lists available at ScienceDirect

Heliyon

journal homepage: www.cell.com/heliyon

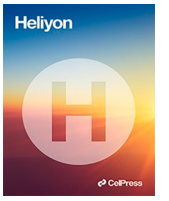

Luteolin reduces cardiac damage caused by hyperlipidemia in Sprague-Dawley rats

Min Dong [a], Yao Luo [a], Yong Lan [b], Qinghua He [c], Lei Xu [d], Zuowei Pei [e,*]

[a] *Department of Cardiology, Beijing Hospital, National Center of Gerontology, Institute of Geriatric Medicine, Chinese Academy of Medical Sciences, Beijing, 100730, China*
[b] *Department of Vascular Surger, Beijing Hospital, National Center of Gerontology, Institute of Geriatric Medicine, Chinese Academy of Medical Sciences, Beijing, 100730, China*
[c] *Department of Endocrinology, Beijing Hospital, National Center of Gerontology, Institute of Geriatric Medicine, Chinese Academy of Medical Sciences, Beijing, 100730, China*
[d] *Department of Neurology, Beijing Hospital, National Center of Gerontology, Institute of Geriatric Medicine, Chinese Academy of Medical Sciences, Beijing, 100730, China*
[e] *Department of Cardiology, Central Hospital of Dalian University of Technology, Dalian, 116033, China*

ARTICLE INFO

Keywords:
Luteolin
Hyperlipidemia
Cardiac damage
Sprague-Dawley rat

ABSTRACT

Objective: Hyperlipidemia is a risk factor for cardiac damage that can lead to many cardiovascular diseases. A recent study reported the cardioprotective effects of luteolin *in vitro* and *in vivo*. In this study, we aimed to investigate the possible protective effects of luteolin against hyperlipidemia-induced cardiac damage in Sprague-Dawley (SD) rats.

Methods: Six-week-old male SD rats were randomly divided into five groups: a normal diet (ND) group; a high-fat diet (HFD) group; and three high-fat diet mixed with luteolin (HFD + LUT) groups, where in a luteolin dosage 50, 100, or 200 mg/kg/day was administered. All groups were fed their respective diets for 12 weeks.

Results: Left ventricular ejection fraction and fractional shortening (parameters of cardiac function) were lower in the HFD + LUT (100 mg/kg/day) group than in the HFD group. Metabolic parameters were lower in the HFD + LUT (100 mg/kg/day) group than in the HFD group. Collagen I, collagen III, and TGF-β expression levels were lower in the cardiac tissues of the HFD + LUT (100 mg/kg/day) group, compared to those of the HFD group. Expression of the profibrotic genes MMP2 and MMP9 was suppressed in the cardiac tissues of the HFD + LUT (100 mg/kg/day) group, compared to those of the HFD group. Furthermore, CD36 and lectin-like oxidized low-density lipoprotein receptor-1 protein levels were lower in the cardiac tissues of the HFD + LUT (100 mg/kg/day) group, compared to those of the HFD group.

Conclusion: These findings would provide new insights into the role of luteolin in hyperlipidemia-induced cardiac damage and contribute to the development of novel therapeutic interventions to treat cardiovascular disease progression.

* Corresponding author. Department of Cardiology, Central Hospital of Dalian University of Technology; Department of Central Laboratory, Central Hospital of Dalian University of Technology, No.826 Xinan Road, 116033, Dalian, China.
E-mail address: pzw_dl@163.com (Z. Pei).

https://doi.org/10.1016/j.heliyon.2023.e17613
Received 13 February 2023; Received in revised form 22 June 2023; Accepted 22 June 2023
Available online 23 June 2023

1. Introduction

Hyperlipidemia can accelerate the development of cardiovascular diseases [1,2]. Several studies have shown that hyperlipidemia accelerates lipid deposition, fibrosis, and chronic inflammation [3,4]. This process was enhanced in the presence of elevated plasma lipid levels. Therefore, the key signaling pathways that decrease myocardial lipid deposition, fibrosis, and inflammation will contribute to a better understanding of these pathophysiological changes, which may lead to new opportunities for disease intervention. When hyperlipidemia occurs, fat deposition or plaque accumulation will occur in the coronary arteries that supply blood to the heart, leading to coronary artery disease development [5]. At the same time, damage to the endothelial cells on the inner wall of the artery leads to thrombosis, which hinders blood flow to the heart [6]. One of the pathogenic factors of coronary heart disease is total cholesterol (TC), which can cause coronary heart disease and damage the heart due to abnormal blood lipid levels [7]. Hyperlipidemia can induce cardiac remodeling, leading to heart failure, ischemic heart disease, and supraventricular and ventricular arrhythmias [8].

Luteolin is a flavonoid found in many herbal extracts, including celery, seeds, perilla leaves, and green peppers. Previous studies have shown that it has potent antioxidant, antifibrotic, anti-inflammatory, and anti-apoptotic activities [9,10]. Earlier studies and clinical trials on luteolin focused on its effects on inflammation and cancer. In recent years, there have been many reports on the cardiovascular effects of luteolin [2]. Luteolin affects heart and vascular vessel diseases. The therapeutic applications of luteolin have been reported in coronary artery disease, atherosclerosis, and heart failure [2,11]. Moreover, luteolin exhibits excellent cardiovascular protective effects by inhibiting inflammatory and oxidative stress mechanisms in cardiovascular diseases [12]. Luteolin also exerts anti-fibrotic effects in the lungs and liver [13–15]. Luteolin provided protection against cardiac fibrosis and hyperoxidative state in angiotensin II-infused rats. In the cardiac tissue, the increased gene expression levels of TGF-β and Nox4 induced by angiotensin II were decreased by luteolin [16].

This study aimed to investigate the protective role of oral luteolin against hyperlipidemia-induced cardiac damage, focusing on the suppressive properties of luteolin against fibrosis and lipid deposition.

2. Results

2.1. Cardiac dysfunction

Echocardiography was examined and evaluated the in each group of Sprague-Dawley (SD) rats (shown in Fig. 1A and B). The high-fat diet (HFD) group showed a marked decrease in left ventricular ejection fraction (LVEF) and fractional shortening (FS); however, these parameters were significantly increased in the HFD with luteolin (HFD + LUT) (100 mg) group.

2.2. Metabolic characterization

Fig. 2 summarizes the metabolic characteristics of SD rats after 12 weeks of dietary treatment. The heart/body weight values [normal diet (ND), 0.11 ± 0.23 mg/g; HFD, 0.2 ± 0.57 mg/g; HFD + LUT (50 mg), 0.23 ± 0.69 mg/g; HFD + LUT (100 mg), 0.13 ± 0.49 mg/g; HFD + LUT (200 mg), 0.18 ± 0.14 mg/g)] and triglyceride (TG) concentration [ND, 0.73 ± 0.14 mmol/L; HFD, 0.52 ± 0.2

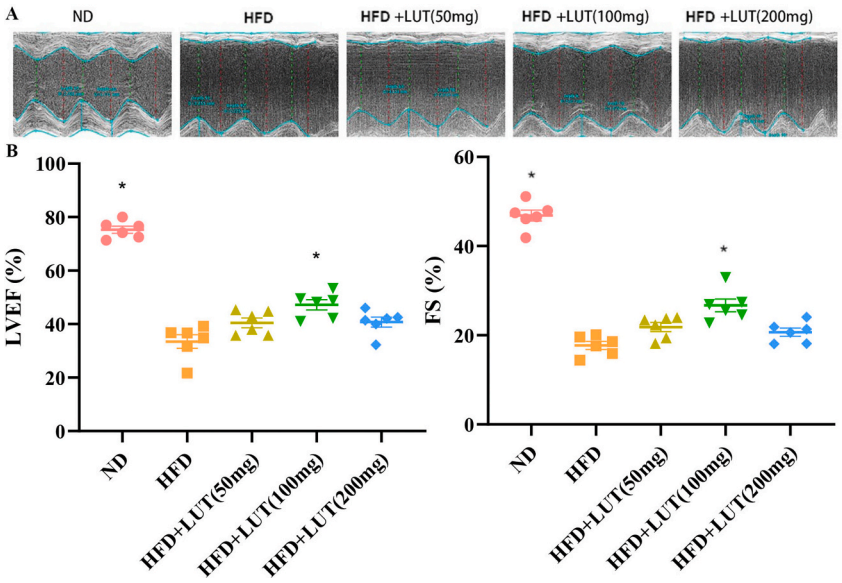

Fig. 1. Luteolin ameliorates hyperlipemia-induced cardiac dysfunction. (A) Representative left ventricular m-mode echocardiography; (B) LVEF and FS were evaluated via echocardiography. Data are presented as mean ± SEM; n = 6 per group. *$P < 0.05$ vs HFD group.

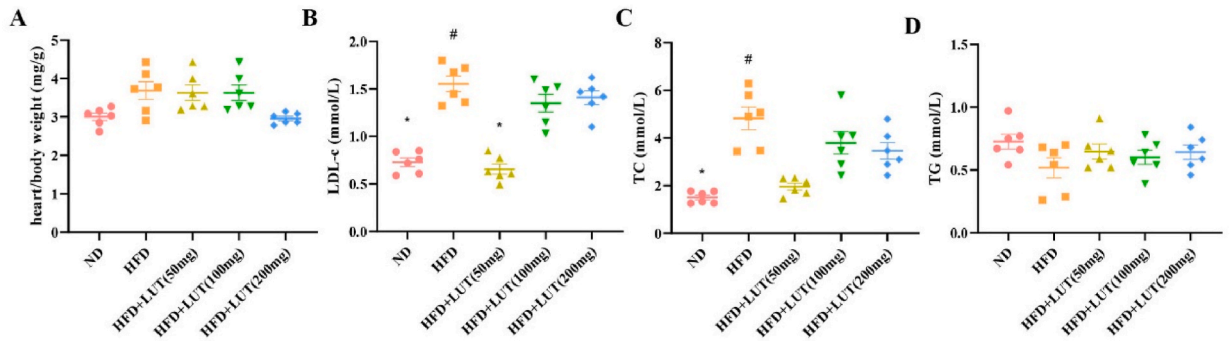

Fig. 2. Metabolic data derived from three groups of rats that were fed different diets. The heart/body weight values and TC, low-density lipoprotein, and TG concentrations of the three groups of rats were evaluated after 12 weeks. Data are presented as the mean ± SEM; n = 6 per group. $^{\#}P < 0.05$ vs ND group, $^{*}P < 0.05$ vs HFD group.

mmol/L; HFD + LUT (50 mg), 0.6 ± 0.14 mmol/L; HFD + LUT (100 mg), 0.65 ± 0.15 mmol/L; HFD + LUT (200 mg), 0.64 ± 0.14 mmol/L] did not differ among the five groups (shown in Fig. 2A and D). The HFD group showed a marked increase in TC and low-density lipoprotein cholesterol (LDL-C) levels compared to the ND group; however, these levels were significantly decreased in the HFD + LUT (100 mg) group. There was no difference between the HFD + LUT (100 mg) and ND groups (Fig. 2B and C). In this study, we found no differences between the HFD and HFD + LUT (50 mg and 200 mg) groups; hence, in subsequent studies, we used the 100 mg dosage of luteolin.

2.3. Effect of luteolin on histopathological cardiac damage

Hematoxylin and eosin (H&E), Masson's trichrome, and PAS staining were performed to evaluate morphological changes in cardiac tissues (Fig. 3A and B). We found that the muscle fibers were disordered, extensively collapsed, degenerated, and showed lipid and collagen deposition in the HFD group. However, this damage was significantly decreased in the HFD + LUT group. These results indicate that luteolin decreased the histopathology of cardiac damage in the HFD group.

2.4. Effect of luteolin on collagen I, collagen III, and TGF-β expression in cardiac tissues

To examine the involvement of profibrotic cytokines in cardiac damage caused by hyperlipidemia, collagen I, collagen III, and TGF-β expression levels were measured by IHC (shown in Fig. 4A and B) and western blotting (shown in Fig. 4C and D). Collagen I, collagen III, and TGF-β expression levels were upregulated in the HFD group compared to those in the ND group. However, this upregulation was attenuated in the HFD + LUT group. These results show that luteolin decreased collagen I, collagen III, and TGF-β protein

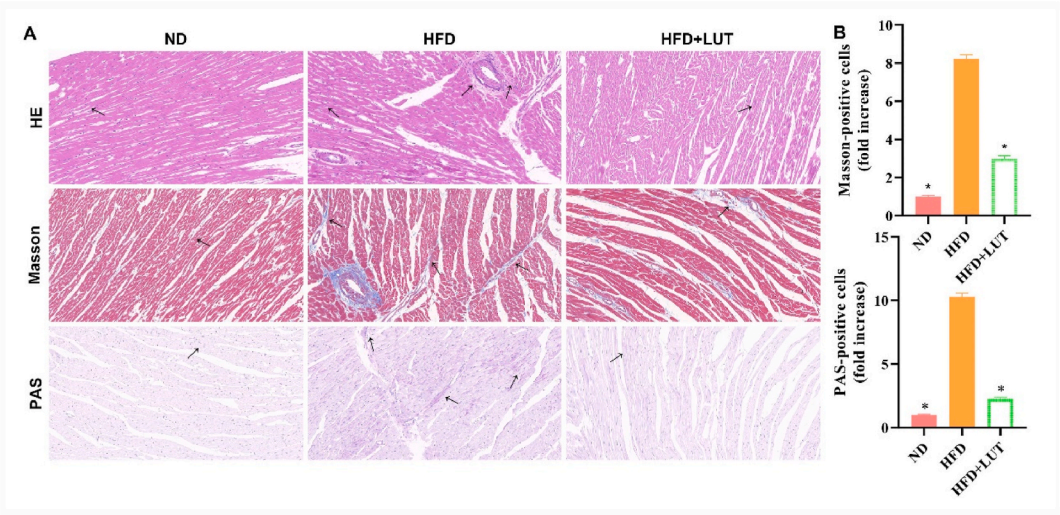

Fig. 3. Morphological changes in the cardiac tissues of three groups of rats fed different diets. (A) H&E, Masson, and PAS staining were performed to assess histopathological damage in the cardiac tissues of rats fed different diets for 12 weeks. Arrows indicate damage. (B) Bar graph showing cells positive under Masson and PAS staining. Data are presented as mean ± SEM; n = 3 per group. $^{*}P < 0.05$ vs HFD group.

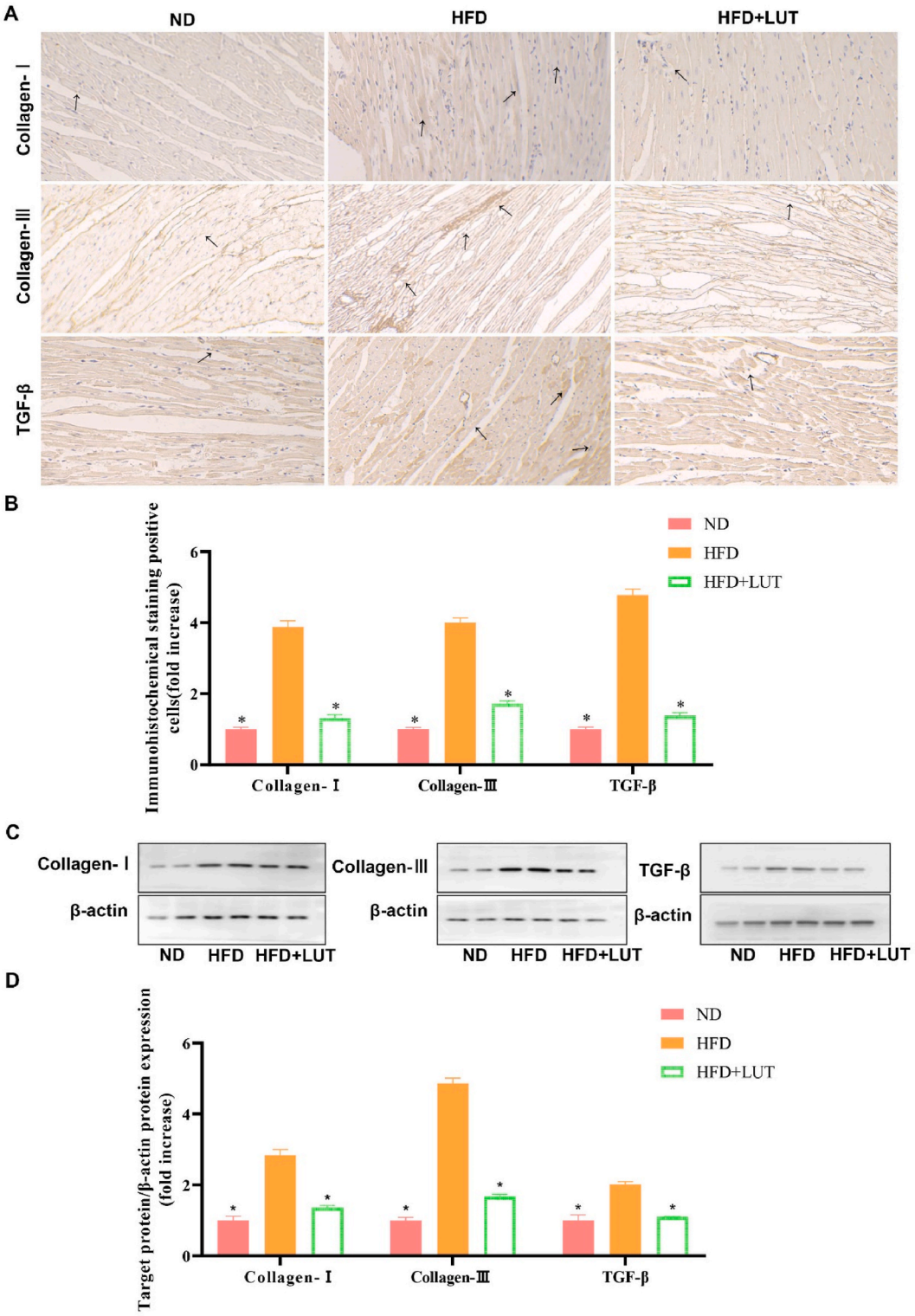

Fig. 4. Collagen I, collagen III, and TGF-β expression in the cardiac tissues of three groups of rats fed different diets. (A) Representative immunohistochemical staining for collagen I, collagen III, and TGF-β. Arrows indicate positively stained cells. (B) Bar graph showing collagen I, collagen III, and TGF-β positive cells. Data are presented as the mean ± SEM; n = 3 in each group. *$P < 0.05$ vs HFD group. (C) Immunoblotting for collagen I, collagen III, and TGF-β protein expression in cardiac tissues. (D) The bar graph shows the quantification of collagen I, collagen III, and TGF-β protein expression. Data are presented as the mean ± SEM; n = 3 in each group. *$P < 0.05$ vs HFD group.

expression in cardiac tissues in the HFD group.

2.5. Effect of luteolin on matrix metalloproteinase 2 (MMP2) and MMP9 expression in cardiac tissues

Real-time PCR and IHC were performed to evaluate MMP2 and MMP9 expression in cardiac tissues (Fig. 5). MMP2 and MMP9 expression was upregulated in the HFD group compared to the ND group (Fig. 5A). However, this upregulation was attenuated in the HFD + LUT group. These results show that luteolin decreased MMP2 and MMP9 expression in the cardiac tissues of the HFD group (Fig. 5B and C).

2.6. Effect of luteolin on CD36 and lectin-like oxidized low-density lipoprotein receptor-1 (LOX-1) protein expression in cardiac tissues

To examine the lipid deposition caused by hyperlipidemia, CD36 and LOX-1 protein expression levels were measured using western blotting and immunohistochemistry (Fig. 6A–D). CD36 and LOX-1 protein expression was upregulated in the HFD group compared with that in the ND group. However, this upregulation was attenuated in the HFD + LUT group. According to the results that luteolin

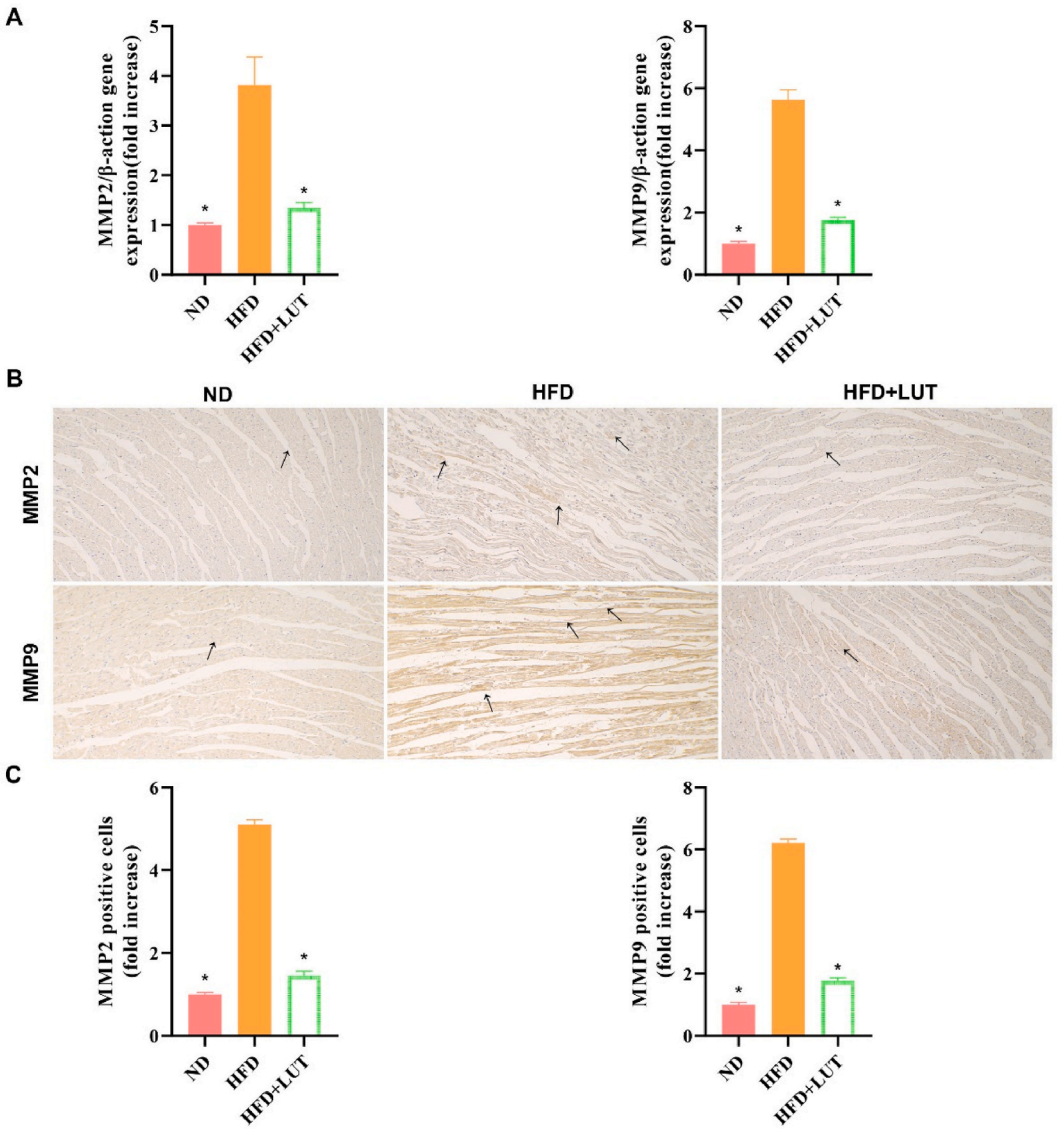

Fig. 5. MMP2 and MMP9 expression in the cardiac tissues of three groups of rats fed different diets. (A) Relative mRNA expression levels of MMP2 and MMP9 in the cardiac tissues of each group were measured after 12 weeks. Data are presented as the mean ± SEM; n = 6 in each group. *$P <$ 0.05 vs HFD group. (B) Representative immunohistochemical staining for MMP2 and MMP9. Arrows indicate positively stained cells. (C) Bar graph showing MMP2 and MMP9 positive cells. Data are presented as the mean ± SEM; n = 3 in each group. *$P < 0.05$ vs HFD group.

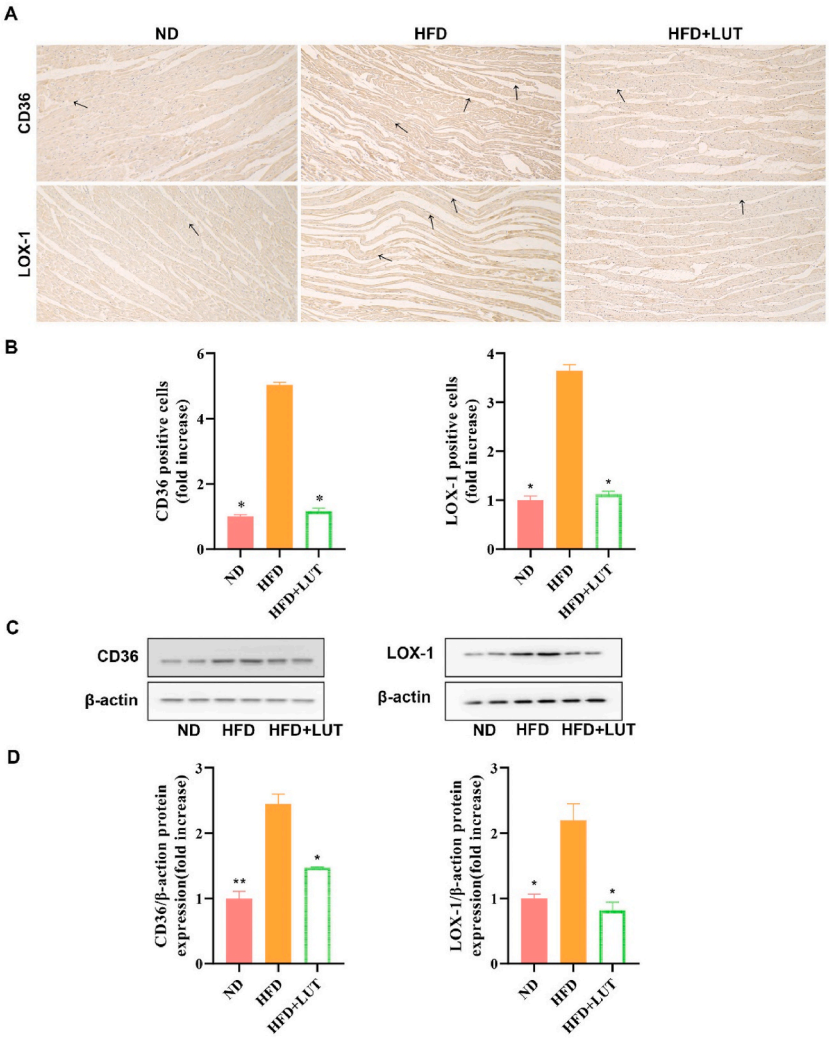

Fig. 6. CD36 and LOX-1 expression in the cardiac tissues of three groups of rats fed different diets. (A) Representative immunohistochemical staining for CD36 and LOX-1. Arrows indicate positively stained cells. (B) Bar graph showing CD36 and LOX-1 positive cells. Data are presented as the mean ± SEM; n = 3 in each group. *$P < 0.05$ vs HFD group. (C) Immunoblotting for CD36 and LOX-1 protein expression in cardiac tissues. (D) The bar graph shows the quantification of CD36 and LOX-1 protein expression. Data are presented as the mean ± SEM; n = 3 in each group. *$P < 0.05$ vs HFD group, **$P < 0.01$ vs HFD group.

decreased CD36 and LOX-1 protein expression of cardiac tissues in the HFD group.

3. Discussion

According to the echocardiography results, luteolin reduced cardiac damage, and this effect was most obvious at a dose of 100 mg/kg/day. Therefore, we performed subsequent experiments using 100 mg/kg/day dose of luteolin.

The present study showed that luteolin prevented cardiac damage, including fibrosis progression and lipid deposition caused by hyperlipidemia (Fig. 7). Regarding the metabolic characteristics of SD rats, the TC and LDL-C levels were significantly higher in the HFD group than in the ND group. However, TC and LDL-C levels were significantly suppressed in the HFD + LUT group compared with those in the HFD group. Our results indicated that luteolin affects cholesterol metabolism. Further studies are required to elucidate these specific mechanisms.

Hyperlipidemia is a well-known risk factor for cardiac fibrosis [17]. Cardiac fibrosis is a common feature of patients with advanced heart failure [18]. Cardiac fibrosis is associated with decreased microvasculature and disruption of normal myocardial structures resulting from excessive deposition of the extracellular matrix. This causes interstitial fibrosis, which enhances intrinsic myocardial stiffness and leads to congestive heart failure [16,19]. TGF-β has been verified to be a potent fibrogenic cytokine [20], which may promote the rapid deposition of the extracellular matrix by enhancing extracellular matrix synthesis and reducing extracellular matrix degradation [21]. Nakayama et al. showed that luteolin provided protection against angiotensin II-induced cardiac fibrosis via TGF-β

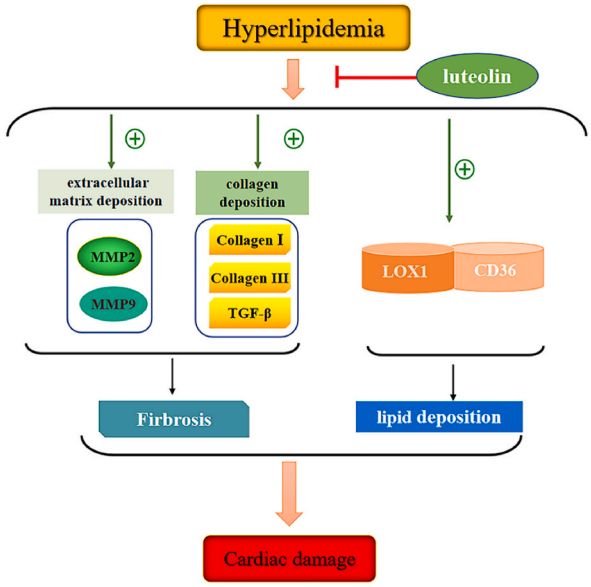

Fig. 7. Schematic representation of the mechanism by which luteolin protects against cardiac damage induced by hyperlipidemia.

expression suppression [16]. To determine the potential mechanisms, we further assessed the effects of luteolin on fibrosis caused by hyperlipidemia. Our results revealed that hyperlipidemia upregulated TGF-β, collagen I, and collagen III protein expression; however, collagen I, collagen III, and TGF-β protein expression was suppressed in the HFD + LUT group. These results agree with those of a study conducted by Ma [22].

TGF-β plays a crucial role in cardiac fibrosis. The pro-fibrotic actions of TGF-β are mediated by the induction of its downstream effectors (i.e., the related genes including collagen I, collagen III, and MMPs) [23–25]. MMPs are key factors that influence the deposition of the extracellular matrix. MMP2 and MMP9 play important roles in cardiac remodeling [26]. The current study elucidated that TGF-β protein levels increased in the HFD group, and this change was accompanied by increases in collagen I, collagen III, MMP2, and MMP9 levels. Treatment with luteolin downregulated MMP2 and MMP9 mRNA expression in cardiac tissues. These results suggest that luteolin therapy could suppress collagen I, collagen III, MMP2, MMP9, and TGF-β expression, which may contribute to the attenuation of cardiac fibrosis in hyperlipidemia.

Cellular lipid homeostasis involves regulation of the influx, synthesis, catabolism, and efflux of lipids. This process is mediated by several independent pathways, including CD36 and LOX-1 [27,28]. CD36 and LOX-1 can mediate oxLDL internalization into macrophages and have been implicated in the pathogenesis of atherosclerosis [29,30]. Ando et al. showed that luteolin inhibits the interaction between macrophages and adipocytes [31]. Our results demonstrated that CD36 and LOX-1 levels were significantly lower in the HFD + LUT group than in the HFD group. Therefore, we propose that luteolin regulates lipid deposition via CD36 and LOX-1.

4. Conclusion

Our study demonstrated that luteolin suppressed cardiac fibrosis (TGF-β, collagen I, collagen III, MMP2, and MMP9) and lipid deposition (CD36 and LOX-1), thereby reducing hyperlipidemia-induced cardiac damage in SD rats. These findings would provide new insights into the role of luteolin in hyperlipidemia-induced cardiac damage and contribute to the development of novel therapeutic interventions to treat cardiovascular disease progression.

5. Materials and methods

5.1. Animals and diets

Six-week-old male SD rats were purchased from Beijing Vital River Laboratories Animal Technology Co., Ltd. (Beijing, China). To evaluate the effect of luteolin on hyperlipidemia, 30 SD rats were divided into five groups: ND (n = 6), high-fat diet (HFD) (n = 6), HFD with luteolin (HFD + LUT) (50 mg/kg/d; n = 6), HFD + LUT (100 mg/kg/d; n = 6), and HFD + LUT (200 mg/kg/d; n = 6). All groups were fed their respective diets for 12 weeks. The high-fat diet was a commercially prepared mouse diet (MD12017) supplemented with 20.0% (w/w) cocoa butter, 1.25% (w/w) cholesterol, 22.5% (w/w) protein, and 45.0% carbohydrates (Jiangsu Mediscience Ltd., Jiangsu, China). At week 12, the rats were anesthetized with 2% isoflurane (Forene®, Abbott), 5 ml of blood was collected from the abdominal aorta, and tissues were obtained for further analysis. All animal experiments were performed per the Guide for the Care and Use of Laboratory Animals and were approved by the Ethics Committee of Dalian Municipal Central Hospital.

5.2. Echocardiography

After 12 weeks of treatment, echocardiography was performed using a Vevo 1100LT micro-ultrasound system (FUJIFILM VisualSonics, Inc.). The rats were anesthetized with isoflurane (1.5–5% v/v in oxygen) and placed in a dorsal recumbent position. The chest was shaved and the transducer was placed directly on the shaved chest wall. Images from M-mode measurements at the papillary muscle level were used to define wall thicknesses and internal diameters at systole and diastole. B-mode and M-mode echoes were used for area and volume measurements, including LVEF and FS.

5.3. Serum analysis

Serum concentrations of TC, LDL-C, and TG were measured using ELISA kits (Westang, Shanghai, China).

5.4. Histological staining

Cardiac tissues were fixed in 10% buffered formalin for 30 min, dehydrated overnight in 75% ethanol, and embedded in paraffin. Serial sections (4 μm) were cut for morphometric analysis of the atherosclerotic lesions. The sections were stained with H&E, Masson's trichrome, and Periodic Acid-Schiff (PAS) for histological analysis. For immunohistochemical staining, the heart sections were deparaffinized and rehydrated. Next, the sections were blocked with 3% H_2O_2 in methanol for 15 min to inactivate the endogenous peroxidases and incubated overnight at 4 ℃ with the primary antibodies: TGF-β (rabbit anti-TGF-β antibody, 1:300; Proteintech, Wuhan, China), collagen I (rabbit anti-collagen I antibody, 1:1000; Proteintech), collagen III (rabbit anti-collagen III antibody, 1:1000; Proteintech), MMP2 (rabbit anti- MMP2 antibody, 1:200; Proteintech), MMP9 (rabbit anti- MMP9 antibody, 1:300; Proteintech), LOX-1 (rabbit anti-LOX-1 antibody, 1:300; Abcam, England, CD36 (rabbit anti-CD36 antibody, 1:500; Proteintech). The sections were then incubated for 30 min at room temperature with a goat anti-rabbit HRP secondary antibody (anti-rabbit Universal Immunohistochemical Detection Kit; Proteintech). All sections were examined with an Olympus B×40 upright light microscope (Olympus, Tokyo, Japan).

5.5. RNA isolation and real-time RT-PCR

Total RNA was isolated from cardiac tissues using the ISOGEN reagent (Nippon Gene, Tokyo, Japan) according to the manufacturer's protocol. Complementary DNA (cDNA) was synthesized from the total RNA using a first-strand cDNA synthesis kit (SuperScript VILO cDNA Synthesis Kit; Life Technologies, Carlsbad, CA, USA) according to the manufacturer's protocol. Gene expression was quantitatively analyzed by real-time RT-PCR using fluorescent SYBR Green technology (Light Cycler; Roche Molecular Biochemicals). To normalize the relative amounts of target genes, β-actin cDNA was amplified and quantified for each cDNA. Table 1 lists the primer sequences.

5.6. Western blot analysis

Cardiac tissues were harvested, and protein extracts were prepared according to established methods. The extracts were separated on sodium dodecyl sulfate-polyacrylamide electrophoresis gels (8–15%) and transferred onto polyvinylidene difluoride (PVDF) membranes (Millipore, Bedford, MA, USA). The PVDF membranes were blocked with 5% milk and incubated with the following primary antibodies at 4 °C overnight: primary antibodies against TGF-β (rabbit *anti*-TGF-β antibody, 1:1000; Proteintech, Wuhan, China), collagen I (rabbit anti-collagen I antibody, 1:1000; Proteintech), collagen III (rabbit anti-collagen III antibody, 1:1000; Proteintech), LOX-1 (rabbit anti-LOX-1 antibody, 1:500; Abcam), CD36 (rabbit anti-CD36 antibody, 1:1000; Proteintech), and β-actin (*anti*-β-actin 1:1000; Cell Signaling Technology). After washing, the membranes were incubated with appropriate secondary antibodies. The membranes were then exposed to an enhanced chemiluminescence reagent (Beyotime Institute of Biotechnology, Hangzhou, China). Emitted light was captured using a Bio-Rad imaging system with a Chemi HR camera 410 and then analyzed using a Gel-Pro Analyzer (version 4.0; Media Cybernetics, Rockville, MD, USA). This analysis was performed independently thrice. Protein levels were expressed as protein/β-actin ratios to minimize loading differences. The relative signal intensity was quantified using the NIH ImageJ software.

5.7. Statistical analysis

All data are presented as the mean ± SEM. Statistical analysis was performed using SPSS software (version 23.0; SPSS Inc., Chicago, IL, USA). Intergroup variation was assessed using one-way ANOVA followed by Tukey's test. The minimum level of significance was $P < 0.05$.

Author contribution statement

Min Dong: Performed the experiments; Contributed reagents, materials, analysis tools or data; Wrote the paper.
Yao Luo: Performed the experiments.
Yong Lan; Qinghua He: Analyzed and interpreted the data.

Table 1
Primer oligonucleotide sequences.

Gene	Primers
MMP2	F:5′- AAAGGAGGGCTGCATTGTGAA-3′ R:5′- CTGGGGAAGGACGTGAAGAGG-3′
MMP9	F:5′-AGGTGCCTCGGATGGTTATCG-3′ R:5′-TGCTTGCCCAGGAAGACGAA-3′
β-actin	F:5′-AACTCCCATTCCTCCACCTT-3′ R:5′-GAGGGCCTCTCTCTTGCTCT-3′

MMP-2, matrix metalloproteinase-2; MMP-9, matrix metalloproteinase-9.

Lei Xu: Contributed reagents, materials, analysis tools or data.
Zuowei Pei: Conceived and designed the experiments; Analyzed and interpreted the data; Wrote the paper.

Funding statement

This study was funded by grant from The Beijing Hospital Research Project (No. BJ-2021-188).

Data availability statement

The datasets used and/or analyzed during the present study are available from the corresponding author on reasonable request.

Declaration of competing interest

The authors declare that they have no known competing financial interests or personal relationships that could have appeared to influence the work reported in this paper.

Appendix A. Supplementary data

Supplementary data to this article can be found online at https://doi.org/10.1016/j.heliyon.2023.e17613.

References

[1] J. Miao, X. Zang, X. Cui, J. Zhang, Autophagy, hyperlipidemia, and atherosclerosis, Adv. Exp. Med. Biol. 1207 (2020) 237–264.
[2] Y. Luo, P. Shang, D. Li, Luteolin: a flavonoid that has multiple cardio-protective effects and its molecular mechanisms, Front. Pharmacol. 8 (2017) 692.
[3] E. Karshovska, Z. Zhao, X. Blanchet, M.M. Schmitt, K. Bidzhekov, O. Soehnlein, et al., Hyperreactivity of junctional adhesion molecule A-deficient platelets accelerates atherosclerosis in hyperlipidemic mice, Circ. Res. 116 (2015) 587–599.
[4] Z. Pei, T. Okura, T. Nagao, D. Enomoto, M. Kukida, A. Tanino, et al., Osteopontin deficiency reduces kidney damage from hypercholesterolemia in Apolipoprotein E-deficient mice, Sci. Rep. 6 (2016), 28882.
[5] J.K. Wang, Y. Li, X.L. Zhao, Y.B. Liu, J. Tan, Y.Y. Xing, et al., Ablation of plasma prekallikrein decreases low-density lipoprotein cholesterol by stabilizing low-density lipoprotein receptor and protects against atherosclerosis, Circulation 145 (2022) 675–687.
[6] J.P. van Geffen, F. Swieringa, K. van Kuijk, B.M.E. Tullemans, F.A. Solari, B. Peng, et al., Mild hyperlipidemia in mice aggravates platelet responsiveness in thrombus formation and exploration of platelet proteome and lipidome, Sci. Rep. 10 (2020), 21407.
[7] A. Alloubani, R. Nimer, R. Samara, Relationship between hyperlipidemia, cardiovascular disease and stroke: a systematic review, Curr. Cardiol. Rev. 17 (2021), e051121189015.
[8] H.X. Zhang, C.S. Zhang, R.Z. Huang, X. Cao, X.Q. Dai, C.Y. Zuo, et al., Oral administration of MnCl(2) attenuated hyperlipidemia-related cardiac remodeling in ApoE(-/-) mice, J. Pharmacol. Sci. 145 (2021) 167–174.
[9] B.C. Zhang, C.W. Zhang, C. Wang, D.F. Pan, T.D. Xu, D.Y. Li, Luteolin attenuates foam cell formation and apoptosis in ox-LDL-stimulated macrophages by enhancing autophagy, Cell. Physiol. Biochem. 39 (2016) 2065–2076.
[10] A.A. Farooqi, G. Butt, S.A. El-Zahaby, R. Attar, U.Y. Sabitaliyevich, J.J. Jovic, et al., Luteolin mediated targeting of protein network and microRNAs in different cancers: focus on JAK-STAT, NOTCH, mTOR and TRAIL-mediated signaling pathways, Pharmacol. Res. 160 (2020), 105188.
[11] X. Hong, X. Zhao, G. Wang, Z. Zhang, H. Pei, Z. Liu, Luteolin treatment protects against renal ischemia-reperfusion injury in rats, Mediat. Inflamm. 2017 (2017), 9783893.
[12] B. Wu, H. Song, M. Fan, F. You, L. Zhang, J. Luo, et al., Luteolin attenuates sepsis-induced myocardial injury by enhancing autophagy in mice, Int. J. Mol. Med. 45 (2020) 1477–1487.
[13] R. Domitrović, H. Jakovac, J. Tomac, I. Sain, Liver fibrosis in mice induced by carbon tetrachloride and its reversion by luteolin, Toxicol. Appl. Pharmacol. 241 (2009) 311–321.
[14] C.Y. Chen, W.H. Peng, L.C. Wu, C.C. Wu, S.L. Hsu, Luteolin ameliorates experimental lung fibrosis both in vivo and in vitro: implications for therapy of lung fibrosis, J. Agric. Food Chem. 58 (2010) 11653–11661.
[15] A. Ghaeni Pasavei, R. Mohebbati, M. Jalili-Nik, H. Mollazadeh, A. Ghorbani, A. Nosrati Tirkani, et al., Effects of Rhus coriaria L. hydroalcoholic extract on the lipid and antioxidant profile in high fat diet-induced hepatic steatosis in rats, Drug Chem. Toxicol. 44 (2021) 75–83.
[16] A. Nakayama, H. Morita, T. Nakao, T. Yamaguchi, T. Sumida, Y. Ikeda, et al., A food-derived flavonoid luteolin protects against angiotensin II-induced cardiac remodeling, PLoS One 10 (2015), e0137106.
[17] A.P. Kalogeropoulos, V.V. Georgiopoulou, J. Butler, From risk factors to structural heart disease: the role of inflammation, Heart Fail. Clin. 8 (2012) 113–123.

[18] A. González, E.B. Schelbert, J. Díez, J. Butler, Myocardial interstitial fibrosis in heart failure: biological and translational perspectives, J. Am. Coll. Cardiol. 71 (2018) 1696–1706.
[19] K.T. Weber, Y. Sun, I.C. Gerling, R.V. Guntaka, Regression of established cardiac fibrosis in hypertensive heart disease, Am. J. Hypertens. 30 (2017) 1049–1052.
[20] N. Frangogiannis, Transforming growth factor-β in tissue fibrosis, J. Exp. Med. 217 (2020), e20190103.
[21] M. Ruiz-Ortega, J. Rodríguez-Vita, E. Sanchez-Lopez, G. Carvajal, J. Egido, TGF-beta signaling in vascular fibrosis, Cardiovasc. Res. 74 (2007) 196–206.
[22] K.L. Ma, J. Liu, J. Ni, Y. Zhang, L.L. Lv, R.N. Tang, et al., Inflammatory stress exacerbates the progression of cardiac fibrosis in high-fat-fed apolipoprotein E knockout mice via endothelial-mesenchymal transition, Int. J. Med. Sci. 10 (2013) 420–426.
[23] M.J. Goumans, P. Ten Dijke, TGF-B signaling in control of cardiovascular function, Cold Spring Harb. Perspect. Biol. 10 (2018).
[24] E. Pardali, P. Ten Dijke, TGFβ signaling and cardiovascular diseases, Int. J. Biol. Sci. 8 (2012) 195–213.
[25] J.N. Zhu, R. Chen, Y.H. Fu, Q.X. Lin, S. Huang, L.L. Guo, et al., Smad3 inactivation and MiR-29b upregulation mediate the effect of carvedilol on attenuating the acute myocardium infarction-induced myocardial fibrosis in rat, PLoS One 8 (2013), e75557.
[26] A.L. Cogni, E. Farah, M.F. Minicucci, P.S. Azevedo, K. Okoshi, B.B. Matsubara, et al., Metalloproteinases-2 and -9 predict left ventricular remodeling after myocardial infarction, Arq. Bras. Cardiol. 100 (2013) 315–321.
[27] K.F. Tseng, P.H. Tsai, J.S. Wang, F.Y. Chen, M.Y. Shen, Sesamol Attenuates renal inflammation and arrests reactive-oxygen-species-mediated IL-1β secretion via the HO-1-induced inhibition of the IKKα/NFκB pathway in vivo and in vitro, Antioxidants (Basel) 11 (2022).
[28] C.K. Glass, J.L. Witztum, Atherosclerosis. the road ahead, Cell 104 (2001) 503–516.
[29] S. Xu, O. Chaudhary, P. Rodríguez-Morales, X. Sun, D. Chen, R. Zappasodi, et al., Uptake of oxidized lipids by the scavenger receptor CD36 promotes lipid peroxidation and dysfunction in CD8(+) T cells in tumors, Immunity 54 (2021) 1561–1577.e1567.
[30] A.J. Kattoor, S.H. Kanuri, J.L. Mehta, Role of ox-LDL and LOX-1 in atherogenesis, Curr. Med. Chem. 26 (2019) 1693–1700.
[31] C. Ando, N. Takahashi, S. Hirai, K. Nishimura, S. Lin, T. Uemura, et al., Luteolin, a food-derived flavonoid, suppresses adipocyte-dependent activation of macrophages by inhibiting JNK activation, FEBS Lett. 583 (2009) 3649–3654.